Journal of Statistical Mechanics: Theory and Experiment
An IOP and SISSA journal

PAPER: Classical statistical mechanics, equilibrium and non-equilibrium

$1/f$ noise in semiconductors arising from the heterogeneous detrapping process of individual charge carriers

Aleksejus Kononovicius* **and Bronislovas Kaulakys**

Institute of Theoretical Physics and Astronomy, Vilnius University, Vilnius, Lithuania
E-mail: aleksejus.kononovicius@tfai.vu.lt

Received 8 July 2024
Accepted for publication 12 October 2024
Published 6 November 2024

Online at stacks.iop.org/JSTAT/2024/113201
https://doi.org/10.1088/1742-5468/ad890b

Abstract. We propose a model of $1/f$ noise in semiconductors based on the drift of individual charge carriers and their interaction with the trapping centers. We assume that the trapping centers are homogeneously distributed in the material. The trapping centers are assumed to be heterogeneous and have unique detrapping rates. We show that uniform detrapping rate distribution emerges as a natural consequence of the vacant trap depths following the Boltzmann distribution, and the detrapping process obeying Arrhenius law. When these laws apply, and if the trapping rate is low in comparison to the maximum detrapping rate, $1/f$ noise in the form of Hooge's relation is recovered. Hooge's parameter, α_{H}, is shown to be a ratio between the characteristic trapping rate and the maximum detrapping rate. The proposed model implies that $1/f$ noise arises from the temporal charge carrier number fluctuations, not from the spatial mobility fluctuations.

Keywords: current fluctuations, fluctuation phenomena, renewal processes, numerical simulations

* Author to whom any correspondence should be addressed.

Contents

J. Stat. Mech. (2024) 113201

1. Introduction

The nature of the $1/f$ noise (often also referred to as low frequency, flicker or pink noise), characterized by power spectral density of $S(f) \sim 1/f^{\beta}$ form (with $0.5 \leqslant \beta \leqslant 1.5$), remains open to discussion despite almost 100 years since the first reports [1–4]. While many materials, devices, and systems exhibit different kinds of fluctuations or noise [4–6], only the white noise and the Brownian noise are well understood from the first principles. White noise is characterized by absence of any temporal correlations, and has a flat power spectral density of $S(f) \sim 1/f^{0}$ form. Examples of the white noise include thermal and shot noise. Thermal noise is known to arise from the random motion of the charge carriers. It occurs at any finite temperature regardless of whether the current flows. Shot noise, on the other hand, is a result of the discrete nature of the charge carriers and the Poisson statistics of waiting times before each individual detection of the charge carrier. The Brownian noise is a temporal integral of the white noise, and thus exhibits no correlations between the increments of the signal, it is characterized by a power spectral density of $S(f) \sim 1/f^{2}$ form.

Theory of $1/f$ noise based on the first principles is still an open problem. $1/f$ noise is of particular interest as it is observed across various physical [7–12], and non-physical [13–16] systems. $1/f$ noise cannot be obtained by the simple procedure of integration, differentiation, or simple transformations of well-understood processes. Also the general mechanism of generating $1/f$ noise has not yet been properly identified, and there is no generally accepted solution to the $1/f$ noise problem.

The oldest explanation for $1/f$ noise involves the superposition of Lorentzian spectra [17–20]. Lorentzian spectral densities themselves may arise from the random telegraph signals [4], and from the Brownian motion with a broad distribution of relaxations [21]. These approaches, as well as many others, are often limited to the specific systems being modeled, or require quite restrictive assumptions to be satisfied [22]. In the recent decades, series of models for the $1/f$ noise based on the specific, autoregressive AR(1), point process [21], and the agent-based model [23, 24], yielding nonlinear stochastic differential equation [25] was proposed (see [26] for a recent review). Another more recent trend relies on scaling properties and nonlinear transformations of signals [27–30]. These models, on the other hand, prove to be rather more abstract, and therefore more similar to the long-range memory models found in the mathematical literature, such as fractional Brownian motion [31, 32] or ARCH models [33, 34]. These and other similar models of $1/f$ noise are hardly applicable to the description and explanation of the mostly observable $1/f$ noise in the semiconductors.

On the other hand, for a homogeneous semiconductor material Hooge proposed an empirical relation for the $1/f$ noise dependence on the parameters of the material [35, 36],

$$S(f) = \bar{I}^2 \frac{\alpha_{\mathrm{H}}}{N f}. \tag{1}$$

Where $\bar{I}$ stands for the average current flowing through the cross-section of the semiconductor material, N is the number of charge carriers, and α_{H} is the titular Hooge parameter. If the current is kept constant, or does not exhibit large fluctuations, Hooge's empirical relation could be rewritten in terms of voltage or resistivity noise, i.e. $S_V(f) = \bar{V}^2 \frac{\alpha_{\mathrm{H}}}{N f}$ or $S_R(f) = \bar{R}^2 \frac{\alpha_{\mathrm{H}}}{N f}$ (here the subscripts emphasize fluctuations of which quantity are being observed). However, we are specifically interested in the case of constant voltage, focusing on the power spectral density of the current fluctuations that are associated with equation (1). There were numerous attempts to derive or explain the structure of the Hooge's relation [37–41]. A more recent derivation of the Hooge's parameter, based on the Poisson generation-recombination process modulated by random telegraph noise, was conducted in [42, 43]. Yet these models, as well as many others, cannot be directly applied to describe and explain the widespread $1/f$ noise in the semiconductors.

Here, we propose a model of $1/f$ noise in semiconductors containing heterogeneous trapping centers. As far as the square of the average current $\bar{I}^2$ is proportional to the squared number of the charge carriers N^2, Hooge's relation implies that the intensity of $1/f$ noise is proportional to the number of charge carriers N. Therefore, as the first approximation we can consider the noise originating from the flow of individual charge carriers. It is known that the drift, and the diffusion, of the charge carriers does not yield $1/f$ noise [4]. Therefore, we consider the drift of the charge carriers interrupted by their entrapment in the trapping centers. We show that, if the detrapping rates of individual trapping centers are heterogeneous and uniformly distributed, $1/f$ noise arises. As an explanation for the uniform detrapping rate distribution, we note that it may arise from the interplay between the Boltzmann distribution of the vacant trap depths (as is observed in various materials [44–47]) and the Arrhenius law (which is often applied in empirical works studying varied activation and detrapping processes in semiconductors [48–51]). In this model, the signal generated by a single charge carrier is similar to the signal composed of non-overlapping rectangular pulses [52]. Here, we derive Hooge's relation, and show that Hooge's parameter is a ratio between the characteristic trapping rate and the maximum detrapping rate. The proportionality between Hooge's parameter and the characteristic trapping rate was reported earlier in quite a few experimental works [53–55]. This result prompts us to suggest that $1/f$ noise in semiconductors arises from the fluctuations in the effective number of charge carriers, not from the spatial fluctuations in mobility.

This paper is organized as follows. In section 2 we introduce a model for $1/f$ noise in the semiconductors based on the trapping-detrapping process of a single charge carrier. In section 3 we address the implications of finite experiments and simulations. Namely, we show that the power spectral density produced by a single charge carrier may exhibit spurious low-frequency cutoff. This cutoff disappears, if the current generated by a large number of charge carriers is considered. Finally, Hooge's empirical relation and Hooge's parameter value for the proposed model is derived in section 4. The main results of the paper are summarized in section 5.

2. Model for $1/f$ noise in a homogeneous semiconductor material

Let us consider a drift of a single charge carrier (e.g. election) through a homogeneous semiconductor material. While the charge carrier is freely moving through the conduction band, it will generate a non-zero contribution to the net current, i.e. $I_1(t) = a$ for t when the charge carrier is free. As the material contains trapping centers, the freely moving charge carrier will eventually get trapped in one of such trapping centers. Let τ_i stand for ith detrapping time (time spent in the trap) and θ_i be ith trapping time (time spent moving). Under these considerations the contribution of single charge carrier to the net current will be composed of gaps (duration corresponds to the respective detrapping time) and pulses (duration corresponds to the respective trapping time). For visual illustration of the single charge carrier trapping-detrapping process and a sample signal see figure 1.

The power spectral density of a signal with rectangular pulses of fixed height is given by [52]

$$S_1(f) = \lim_{T\to\infty} \left\langle \frac{2}{T} \left| \int_0^T I_1(t)\, \mathrm{e}^{-2\pi \mathrm{i} f t}\, \mathrm{d}t \right| \right\rangle = \frac{a^2 \bar{\nu}}{\pi^2 f^2} \mathrm{Re}\left[\frac{(1-\chi_\theta(f))(1-\chi_\tau(f))}{1-\chi_\theta(f)\chi_\tau(f)} \right]. \tag{2}$$

In the above T stands for observation time (duration of the signal), which is assumed to approach infinity [52], $\chi_\tau(f)$ and $\chi_\theta(f)$ stand for the characteristic functions of the respective detrapping and trapping time distributions, while $\bar{\nu}$ is the mean number of pulses per unit time. For the ergodic processes, and given a long observation time T, the value of $\bar{\nu}$ is trivially derived from the mean trapping and detrapping times, i.e. $\bar{\nu} = \frac{1}{\langle\theta\rangle + \langle\tau\rangle}$. For the nonergodic processes, or if the observation time T is comparatively short, the expected value of $\bar{\nu}$ can be derived from the means of the appropriately truncated distributions, or it may be defined purely empirically, i.e. $\bar{\nu} = K/T$ (here K is the number of observed pulses).

Typically when trapping–detrapping processes are considered [4, 9] it is assumed that both τ_i and θ_i are sampled from the exponential distributions with rates γ_τ and γ_θ, respectively. Characteristic function of the exponential distribution with an event

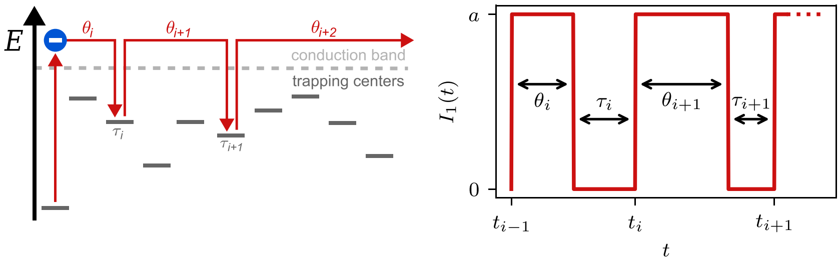

Figure 1. Visualization of the single charge carrier trapping-detrapping process (left) and a sample single charge carrier contribution to the net current (right). Relevant notation: τ_i is the detrapping time (gap duration), θ_i is the trapping time (pulse duration), a is the height of the pulses (single free charge carrier contribution to the net current), t_i is the time of ith detrapping event.

rate γ, is given by

$$\chi(f) = \int_0^\infty \gamma \mathrm{e}^{2\pi \mathrm{i} f\tau - \gamma\tau}\, \mathrm{d}\tau = \frac{\gamma}{\gamma - 2\pi \mathrm{i} f}. \tag{3}$$

Inserting equation (3) as the characteristic function for both trapping and detrapping time distributions into equation (2) yields a Lorentzian power spectral density [4]. Notably, there were prior works which have examined the case when τ_i, θ_i, or both are sampled from distributions with power-law tails [42, 43, 52, 56–59]. Under the power-law distribution assumption, it was shown $S(f) \sim 1/f^\beta$ dependence can be recovered.

Here, let us assume that the trapping centers are heterogeneous. Each of them has their own unique depth, or detrapping (activation) energy, $E_a^{(i)}$. As is commonly observed [48–51], let us assume that the detrapping process obeys Arrhenius law

$$\gamma_\tau^{(i)} = A \exp\left[-\frac{E_a^{(i)}}{k_\mathrm{B}\Theta}\right]. \tag{4}$$

To obtain the overall detrapping time distribution we first need to establish the distribution of detrapping energies. Not all trapping centers will participate in the trapping-detrapping process at all times. Because charge carrier first needs to be trapped, before being detrapped, only vacant trapping centers will participate in the process. In experimental literature [44–47] it is well established that vacant trap level depths (their activation energies) reasonably well follow the Boltzmann distribution

$$p\left[E_a^{(i)}\right] = C_N \exp\left[-\frac{E_a^{(i)}}{k_\mathrm{B}\Theta}\right]. \tag{5}$$

In the above C_N stands for the normalization constant. Notably, this result also follows directly from the Fermi–Dirac statistics under the assumption that trap level degeneracy is constant in respect to activation energy. Then, from the conservation of the probability density, it follows that the distribution of detrapping rates would be uniform

$$p\left[\gamma_\tau^{(i)}\right] = \frac{p\left[E_a^{(i)}\right]}{\left|\frac{\mathrm{d}\,c}{\mathrm{d}\,E_a^{(i)}}\right|} = \frac{C_N \exp\left[-\frac{E_a^{(i)}}{k_\mathrm{B}\Theta}\right]}{\frac{A}{k_\mathrm{B}\Theta}\exp\left[-\frac{E_a^{(i)}}{k_\mathrm{B}\Theta}\right]} = \text{const.} \tag{6}$$

It is important to note that other physical mechanisms could also imply uniform distribution of the detrapping rates as long as $\frac{p(\eta)}{\left|\frac{\mathrm{d}\gamma_\tau^{(i)}}{\mathrm{d}\eta}\right|} = \text{const}$ (here η is some generic physical quantity which would impact the detrapping process).

Let $\gamma_\tau^{(i)}$ be uniformly distributed in $[\gamma_\mathrm{min}, \gamma_\mathrm{max}]$. Then it can be shown that the probability density function of the detrapping time distribution is given by

$$\begin{aligned} p(\tau) &= \frac{1}{\gamma_\mathrm{max} - \gamma_\mathrm{min}} \int_{\gamma_\mathrm{min}}^{\gamma_\mathrm{max}} \gamma_\tau \exp(-\gamma_\tau \tau)\,\mathrm{d}\,\gamma_\tau \\ &= \frac{(1+\gamma_\mathrm{min}\tau)\exp(-\gamma_\mathrm{min}\tau) - (1+\gamma_\mathrm{max}\tau)\exp(-\gamma_\mathrm{max}\tau)}{(\gamma_\mathrm{max} - \gamma_\mathrm{min})\,\tau^2}. \end{aligned} \tag{7}$$

This probability density function saturates for the short detrapping times, $\tau \ll \frac{1}{\gamma_\mathrm{max}}$. For the longer detrapping times, $\tau \gg \frac{1}{\gamma_\mathrm{min}}$, it decays as an exponential function. In the intermediate value range, $\frac{1}{\gamma_\mathrm{max}} \ll \tau \ll \frac{1}{\gamma_\mathrm{min}}$, this probability density function has the τ^{-2} asymptotic behavior, which is already known to lead to $1/f$ noise [52, 56–58]. The benefit of this formulation is that it allows to see how the τ^{-2} asymptotic behavior can emerge in homogeneous semiconductors. Experimentally τ^{-2} asymptotic behavior is observable in quantum dots, nanocrystal, nanorod, and other semiconductors [60–63], with the detrapping times ranging from picoseconds to several months. The asymptotic behavior of equation (7) can be examined in figure 2 where it is represented by a red curve. Figure 2 also highlights contributions of some of the individual trapping centers, detrapping time distributions of which are plotted as dashed black curves.

Unlike the simple power-law distribution, this detrapping time distribution does not require the introduction of any arbitrary cutoffs. Also the parameters of this detrapping time distribution have explicit physical meaning. Furthermore, the statistical moments are well-defined and have compact analytical forms. The mean of the distribution is given by

$$\langle \tau \rangle = \frac{1}{\gamma_\mathrm{max} - \gamma_\mathrm{min}} \ln\left(\frac{\gamma_\mathrm{max}}{\gamma_\mathrm{min}}\right). \tag{8}$$

Higher order moments also exist and can be easily derived.

The characteristic function of the detrapping time distribution can be obtained either by calculating Fourier transform of equation (7), or by averaging over the characteristic functions of the exponential distribution, equation (3). Both approaches lead to the

J. Stat. Mech. (2024) 113201

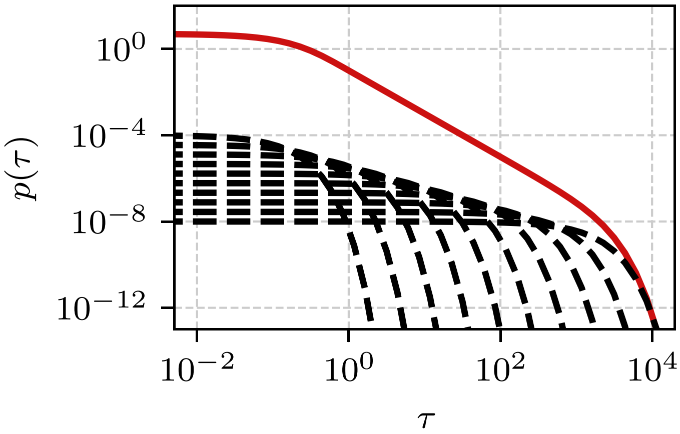

Figure 2. Probability density function of the detrapping time distribution under the assumption that detrapping rates of individual trapping centers are uniformly distributed (red curve), equation (7). The probability density function was calculated for $\gamma_{\min} = 10^{-3}$, and $\gamma_{\max} = 10$ case. Black dashed curves correspond to the exponential probability density functions of the detrapping times from the individual trapping centers with fixed rates: $\gamma_\tau = 10^{-3}$, 2.78×10^{-3}, 7.74×10^{-3}, 2.15×10^{-2}, 5.99×10^{-2}, 1.67×10^{-1}, 4.64×10^{-1}, 1.29, 3.59, and 10. Normalization of the exponential probability density functions was adjusted for the visualization purposes, but it remains proportional to their respective contributions.

same expression, but the latter approach is quicker

$$\chi_\tau(f) = \frac{1}{\gamma_{\max}-\gamma_{\min}}\int_{\gamma_{\min}}^{\gamma_{\max}} \frac{\gamma_\tau}{\gamma_\tau - 2\pi\mathrm{i}f}\,\mathrm{d}\gamma_\tau = 1 + \frac{2\pi\mathrm{i}f}{\gamma_{\max}-\gamma_{\min}}\ln\left(\frac{\gamma_{\max}-2\pi\mathrm{i}f}{\gamma_{\min}-2\pi\mathrm{i}f}\right). \tag{9}$$

If the interval of the possible detrapping rates is broad $\gamma_{\min} \ll \gamma_{\max}$, then for $\gamma_{\min} \ll 2\pi f \ll \gamma_{\max}$ the characteristic function can be approximated by

$$\chi_\tau(f) \approx 1 + \frac{2\pi\mathrm{i}f}{\gamma_{\max}}\ln\left(1+\frac{\mathrm{i}\gamma_{\max}}{2\pi f}\right) \approx 1 - \frac{2\pi f}{\gamma_{\max}}\left[\frac{\pi}{2} - \mathrm{i}\ln\left(\frac{2\pi f}{\gamma_{\max}}\right)\right]. \tag{10}$$

Inserting equation (10) into equation (2) we have

$$S_1(f) = \frac{2a^2\bar{\nu}}{\pi\gamma_{\max}f}\mathrm{Re}\left[\frac{(1-\chi_\theta(f))\left[\frac{\pi}{2}-\mathrm{i}\ln\left(\frac{2\pi f}{\gamma_{\max}}\right)\right]}{1-\chi_\theta(f)\left\{1-\frac{2\pi f}{\gamma_{\max}}\left[\frac{\pi}{2}-\mathrm{i}\ln\left(\frac{2\pi f}{\gamma_{\max}}\right)\right]\right\}}\right]. \tag{11}$$

Assuming that $\frac{2\pi f}{\gamma_{\max}}[\frac{\pi}{2} - \mathrm{i}\ln(\frac{2\pi f}{\gamma_{\max}})] \ll 1$, which is supported by an earlier assumption that $2\pi f \ll \gamma_{\max}$, allows to simplify the above to

$$S_1(f) \approx \frac{a^2\bar{\nu}}{\gamma_{\max}f}. \tag{12}$$

This approximation should hold well for $\gamma_{\min} \ll 2\pi f \ll \gamma_{\max}$, and should not depend on the explicit form of $\chi_\theta(f)$ unless $\chi_\theta(f) \approx 1$ for at least some of the frequencies in the range.

J. Stat. Mech. (2024) 113201

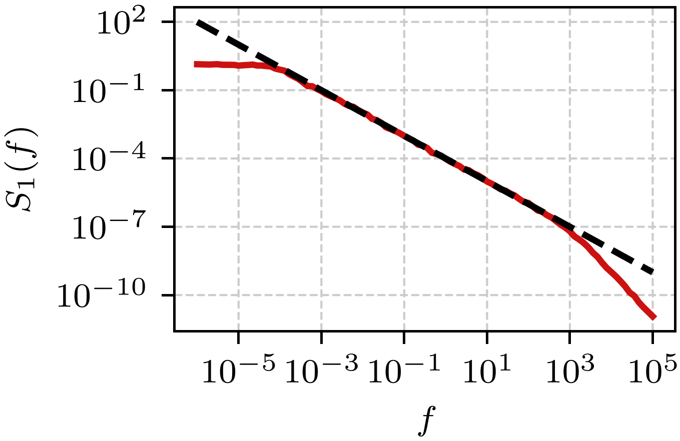

Figure 3. Power spectral density of the simulated signal (red curve) and its analytical approximation by equation (12) (black dashed curve). Simulated power spectral density was obtained by averaging over 10^2 realizations. Simulation parameters: $T = 10^6$, $\gamma_{\min} = 10^{-4}$, $\gamma_{\max} = 10^4$, $a = 1$, $\gamma_\theta = 1$.

Let us examine a specific case when the trapping centers are uniformly distributed within the material, and therefore the trapping process can be assumed to be a homogeneous Poisson process. Inserting the characteristic function of the exponential distribution, equation (3), as the characteristic function of the trapping time distribution into equation (2) yields

$$S_1(f) = \frac{4a^2\bar{\nu}}{\gamma_\theta^2} \operatorname{Re}\left[\frac{1}{1 - \chi_\tau(f) - \frac{2\pi \mathrm{i} f}{\gamma_\theta}}\right]. \tag{13}$$

Then inserting the characteristic function of the proposed detrapping time distribution, equation (10), into equation (13) yields

$$S_1(f) = \frac{a^2\bar{\nu}\gamma_{\max}}{\gamma_\theta^2 f} \times \frac{1}{\left(\frac{\pi}{2}\right)^2 + \left[\frac{\gamma_{\max}}{\gamma_\theta} + \ln\left(\frac{2\pi f}{\gamma_{\max}}\right)\right]^2}. \tag{14}$$

If the maximum detrapping rate is large in comparison to the trapping rate, i.e. $\frac{\gamma_{\max}}{\gamma_\theta} \gg \frac{\pi}{2}$ and $\frac{\gamma_{\max}}{\gamma_\theta} \gg -\ln(\frac{2\pi f}{\gamma_{\max}})$, then we recover equation (12). In figure 3 the power spectral density of a simulated signal with comparatively large detrapping rates is shown as a red curve. We have chosen observation time T to allow us to show three regimes of the power spectral density: white noise cutoff for $2\pi f \ll \gamma_{\min}$, $1/f$ noise for $\gamma_{\min} \ll 2\pi f \ll \gamma_{\max}$ and Brown noise for $\gamma_{\max} \ll 2\pi f$. Longer or similar observation times would yield similar power spectral density.

3. Low-frequency cutoff in finite experiments

The obtained approximation, equation (12), holds in the infinite observation time limit (single signal of infinite duration T) or the infinite number of experiments limit (infinitely many signals with finitely long observation time T). If either of the limits does not hold, then the range of frequencies over which the pure $1/f$ noise is observed becomes narrower. In the finite experiments the process will not reach a steady state, and therefore the cutoff frequencies will depend not on the model parameter values $\gamma_{\min}$ and $\gamma_{\max}$, but on the smallest and the largest $\gamma_\tau^{(i)}$ values actually observed during the experiment. The difference between $\gamma_{\max}$ and the largest $\gamma_\tau^{(i)}$ is negligible, because the pure $1/f$ noise will be observed only if $\gamma_{\max}$ is a relatively large number. On the other hand the relative difference between $\gamma_{\min}$ and smallest $\gamma_\tau^{(i)}$ might not be negligible. Let us estimate the expected value of the smallest $\gamma_\tau^{(i)}$ in a finite experiment.

In the model introduced in the previous section $\gamma_\tau^{(i)}$ is sampled from the uniform distribution with $[\gamma_{\min}, \gamma_{\max}]$ range of possible values. It is known that, for x_i sampled from the uniform distribution with $[0,1]$ range of possible values, the smallest x_i observed in the sample of size K is distributed according to the Beta distribution with the shape parameters $\alpha_1 = 1$ and $\alpha_2 = K$ [64]. Thus the expected value of the smallest x_i is given by

$$\langle \min \{x_i\}_K \rangle = \frac{\alpha_1}{\alpha_1 + \alpha_2} = \frac{1}{K+1}. \tag{15}$$

Rescaling the range of possible values to $[\gamma_{\min}, \gamma_{\max}]$ yields

$$\gamma_{\min}^{(\mathrm{eff})} = \left\langle \min \left\{ \gamma_\tau^{(i)} \right\}_K \right\rangle = \frac{\gamma_{\max} - \gamma_{\min}}{K+1} + \gamma_{\min}. \tag{16}$$

As K corresponds to the number of pulses in the signal, we have that $K = \bar{\nu} T = \frac{T}{\langle\theta\rangle + \langle\tau\rangle}$ and

$$\gamma_{\min}^{(\mathrm{eff})} = (\gamma_{\max} - \gamma_{\min}) \frac{\langle\theta\rangle + \langle\tau\rangle}{\langle\theta\rangle + \langle\tau\rangle + T} + \gamma_{\min}. \tag{17}$$

In the above $\langle\theta\rangle$ is effectively a model parameter as it is trivially given by $\langle\theta\rangle = \frac{1}{\gamma_\theta}$, while $\langle\tau\rangle$ is a derived quantity which has a more complicated dependence on the model parameters $\gamma_{\min}$ and $\gamma_{\max}$ (see equation (8)). If the range of possible $\gamma_\tau^{(i)}$ values is broad, i.e. $\gamma_{\max} \gg \gamma_{\min}$, we have

$$\gamma_{\min}^{(\mathrm{eff})} \approx \gamma_{\max} \frac{\gamma_{\max} \langle\theta\rangle + \ln \frac{\gamma_{\max}}{\gamma_{\min}}}{\gamma_{\max} (\langle\theta\rangle + T) + \ln \frac{\gamma_{\max}}{\gamma_{\min}}} + \gamma_{\min}. \tag{18}$$

The above applies to the ergodic case with $\gamma_{\min} \gg 1/T$. In the nonergodic case, for $\gamma_{\min} \lesssim 1/T$, it would impossible to distinguish between the cases corresponding to the different $\gamma_{\min}$ values. Therefore, for the nonergodic case, $\gamma_{\min}$ can be replaced by $1/T$ yielding

J. Stat. Mech. (2024) 113201

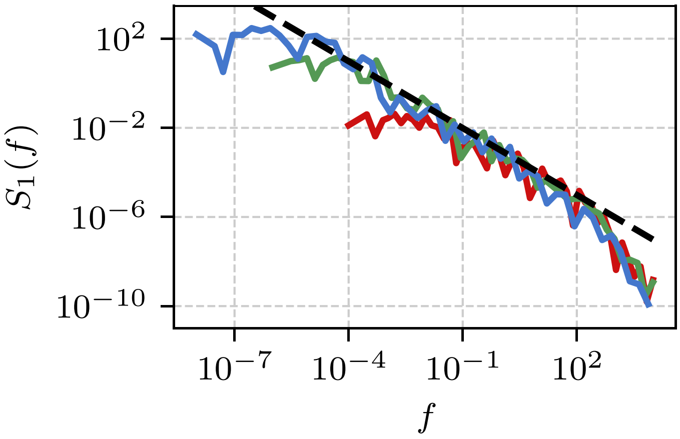

Figure 4. The effect of increasing the observation time T on the obtained power spectral density. Dashed black curve corresponds to equation (12). Simulation parameters: $a=1$, $\gamma_\theta=1$, $\gamma_{\min}=0$, $\gamma_{\max}=10^3$, $T=10^4$ (red curve), 10^6 (green curve), and 10^8 (blue curve).

$$\gamma_{\min}^{(\mathrm{eff})} \approx \gamma_{\max}\frac{\gamma_{\max}\langle\theta\rangle+\ln(\gamma_{\max}T)}{\gamma_{\max}(\langle\theta\rangle+T)+\ln(\gamma_{\max}T)}+\frac{1}{T}\approx\frac{1+\gamma_{\max}\langle\theta\rangle+\ln(\gamma_{\max}T)}{T}. \tag{19}$$

For relatively long trapping times, $\langle\theta\rangle \gg \frac{\ln(\gamma_{\max}T)}{\gamma_{\max}}$, we have that

$$\gamma_{\min}^{(\mathrm{eff})} \approx \frac{1+\gamma_{\max}\langle\theta\rangle}{T}\approx\frac{\gamma_{\max}}{\gamma_\theta T}. \tag{20}$$

From the above, it follows that low-frequency cutoff is always present in singular experiments with one charge carrier, and with finite observation time T. The cutoff will be observed at a frequency close to $\gamma_{\min}^{(\mathrm{eff})}$. As can be seen in figure 4, the cutoff moves to the lower frequencies as T increases, the power spectral density is flat for the lowest observable natural frequencies, $\frac{1}{T}<f\lesssim\frac{\gamma_{\max}}{\gamma_\theta T}$.

If multiple independent experiments (let R be the number of experiments) with finite observation time T are performed and the obtained spectral densities are averaged, then the total number of observed pulses increases by a factor of R yielding

$$\gamma_{\min}^{(\mathrm{eff})} = (\gamma_{\max}-\gamma_{\min})\frac{\langle\theta\rangle+\langle\tau\rangle}{\langle\theta\rangle+\langle\tau\rangle+RT}+\gamma_{\min}\approx\frac{\gamma_{\max}\langle\theta\rangle}{RT}+\frac{1}{T}=\frac{R+\gamma_{\max}\langle\theta\rangle}{RT}. \tag{21}$$

For $R\gg\gamma_{\max}\langle\theta\rangle$, no low-frequency cutoff will be noticeable. As shown in figure 5, low-frequency cutoff disappears as the experiments are repeated and the obtained power spectral densities are averaged.

We have derived equation (12) considering the current generated by a single charge carrier. In many experiments the number of charge carriers N will be large, $N\gg1$. Consequently, from the Wiener–Khinchin theorem [4] it follows that performing independent experiments is equivalent to observing independent charge carriers. Therefore for $N\gg\gamma_{\max}\langle\theta\rangle$ no low-frequency cutoff will be noticeable. Though in this case, the

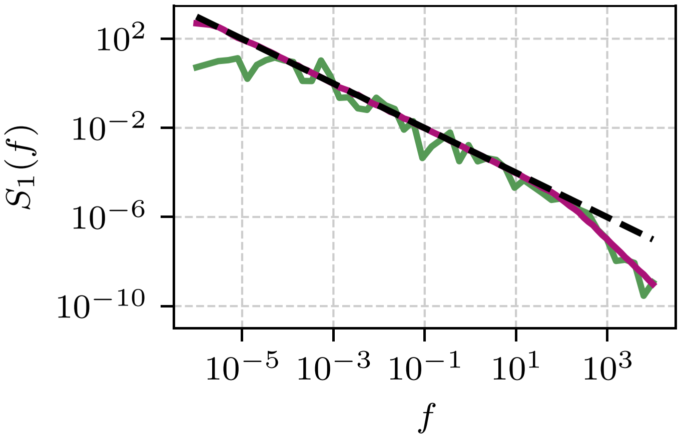

Figure 5. The effect of averaging over repeated experiments on the obtained power spectral density: $R = 1$ (green curve), $R = 10^3$ (magenta curve). Dashed black curve corresponds to equation (12). Simulation parameters, with exception to R, are the same as for the green curve from figure 4.

power spectral densities of the signals generated by single charge carriers add up instead of averaging out, yielding a minor generalization of equation (12)

$$S_N(f) \approx \frac{N a^2 \bar{\nu}}{\gamma_{\max} f}. \tag{22}$$

In the above $\bar{\nu}$ is strictly the mean number of pulses per unit time generated by a single charge carrier.

As can be seen in figure 6(a), the signal generated by multiple independent charge carriers is no longer composed of non-overlapping pulses, although it retains discrete nature as individual charges drift freely or are trapped by the trapping centers. The amplitude and the slope of the power spectral density are well predicted by equation (22) (as seen in figure 6(c)). The distribution of the signal's amplitude would be expected to follow the Binomial distribution with sample size N and success probability (probability that the charge carrier is free)

$$p_{\mathrm{F}} = \frac{\langle\theta\rangle}{\langle\theta\rangle + \langle\tau\rangle} \approx 1 - \frac{\langle\tau\rangle}{\langle\theta\rangle}. \tag{23}$$

The fit by the Binomial distribution shown in figure 6(b) is not perfect, because the nonergodic case is simulated and $\langle\tau\rangle$ is ill-defined, but predicts the overall shape of the probability distribution rather well. For $\gamma_{\min} \gg 1/T$ the fit would be much better. Notably, with larger N and under noisy observation, the Binomial distribution predicted by the model will quickly become indistinguishable from the Gaussian distribution. While in some cases $1/f$ noise is known to behave as a non-Gaussian process, most often it is found to exhibit Gaussian fluctuations [4, 65, 66]. The duration of the reported simulation was chosen arbitrarily, based on the technical considerations. Specifically, we have opted to make 2^{26} observations of the process with sampling period of $\Delta t = 10^{-4}$.

J. Stat. Mech. (2024) 113201

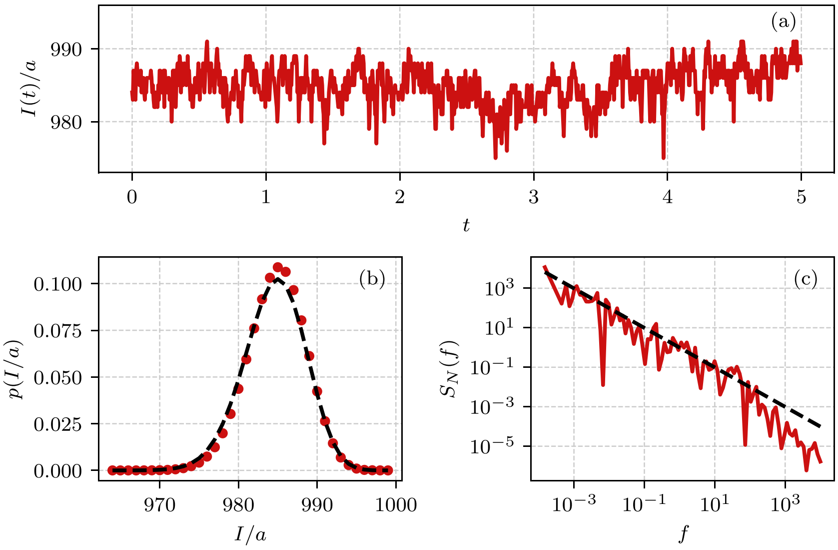

Figure 6. Results of a single simulation with large number of charge carriers N and finite duration T: excerpt of a signal generated by 10^3 independent charge carriers (a), the probability mass function of the amplitude of the signal (b), and the power spectral density of the signal (c). Red curves represent results of numerical simulation, while dashed black curves provide theoretical fits: (b) binomial probability mass function with $p_{\mathrm{F}} \approx 0.984$ and $N = 10^3$, (c) the power spectral density approximation equation (22). Simulation parameters: $R = 1$, $N = 10^3$, $T = 2^{26} \cdot 10^{-4} = 6710.8864$, $a = 1$, $\gamma_\theta = 1$, $\gamma_{\min} = 0$, $\gamma_{\max} = 10^3$.

Notably, [67] also discusses a spurious low-frequency cutoff that could be observed in single particle experiments. Of the $1/f$ noise models considered in [67] superimposed random telegraph signals and blinking quantum dot models are the most comparable to the model presented here. In [67] each of the superimposed random telegraph signals was assumed to be characterized by their own Poissonian switching rate $\gamma = \gamma_\theta = \gamma_\tau$ between the 'on' and 'off' states. It was shown that the conditional power spectral density (requiring a certain minimum number of pulses, $K_{\min}$, to be observed) exhibits low-frequency cutoff at $f_{\mathrm{c}} \sim K_{\min}/T$. In our simulations, we typically observe a large number of pulses, $K \approx \gamma_\theta T$, and should therefore observe the cutoff at $f_{\mathrm{c}} \sim \gamma_\theta$, but instead, we observe that the cutoff frequency scales as $1/\gamma_\theta$. The nature of the cutoff is different in the model introduced here. The other, blinking quantum dot, model does not predict low-frequency cutoff, only the ageing effect, which for the pure $1/f$ noise will not be noticeable [52].

4. Derivation of Hooge's empirical relation and Hooge's parameter

It is straightforward to see that we can rewrite equation (22) in the form of Hooge's empirical relation, equation (1), if we define Hooge's parameter as

$$\alpha_{\mathrm{H}} = \frac{N^2 a^2 \bar{\nu}}{\gamma_{\max} \bar{I}^2}. \tag{24}$$

Further we show that the straightforward expression above can be simplified, and given a more compact form.

As the height of the pulses a corresponds to the current generated by a single charge carrier, we have

$$a = \frac{q v_{\mathrm{c}}}{L}, \tag{25}$$

where q stands for the charge held by the carrier, v_{c} is the free drift velocity between the trappings (which will be much smaller than the thermal velocity of the charge carriers), and L is the length of the material. Expression for a can be rewritten in terms of the average current flowing through the cross-section of the material σ_M

$$\bar{I} = \sigma_M n q v_{\mathrm{d}}, \tag{26}$$

where n stands for the density of the charge carriers (i.e. $n = \frac{N}{L\sigma_M}$), and v_{d} is the average drift velocity of the charge carriers. The average drift velocity is related to the free drift velocity via the fraction of time the charge carrier spends drifting

$$v_{\mathrm{d}} = \frac{\langle \theta \rangle}{\langle \theta \rangle + \langle \tau \rangle} v_{\mathrm{c}} = \bar{\nu} \langle \theta \rangle v_{\mathrm{c}}. \tag{27}$$

Consequently we have

$$a = \frac{\bar{I}}{N \bar{\nu} \langle \theta \rangle}. \tag{28}$$

Inserting equation (28) into equation (24) yields the expression of the Hooge's parameter in terms of the characteristic trapping rate and the maximum detrapping rate, assuming that the trapping times are comparatively long $\langle \theta \rangle \gg \langle \tau \rangle$,

$$\alpha_{\mathrm{H}} = \frac{1}{\bar{\nu} \langle \theta \rangle^2 \gamma_{\max}} \approx \frac{\gamma_\theta}{\gamma_{\max}} = \frac{\langle \tau_{\min} \rangle}{\langle \theta \rangle}. \tag{29}$$

In the above $\langle \tau_{\min} \rangle = \frac{1}{\gamma_{\max}}$ is the expected detrapping time generated when a charge carrier is trapped by the shallowest trapping center. The purer materials (i.e. ones with lower trapping center density n_{c}) will have lower α_{H} values, as the trapping rate is given by $\gamma_\theta = \langle \sigma_{\mathrm{c}} v_{\mathrm{t}} \rangle n_{\mathrm{c}}$ (here v_{t} is the thermal velocity of the charge carriers, and σ_{c} is the trapping cross-section). The proportionality $\alpha_{\mathrm{H}} \propto \gamma_\theta$ was previously reported in [53–55], providing experimental support to equation (29).

Consequently the approximations for the power spectral density generated by the proposed model, equations (12) and (22), can be rewritten in the same form as Hooge's empirical relation. Inserting equation (29) into equation (1) yields

$$S_N(f) = \bar{I}^2 \frac{\gamma_\theta}{\gamma_{\max} N f}. \tag{30}$$

This expression appears to imply that the process under consideration is stationary, but this is not true as the average current $\bar{I}$ is proportional to the number of pulses per

J. Stat. Mech. (2024) 113201

unit time $\bar{\nu}$, which in the $\gamma_{\text{min}} \to 0$ limit is a function of the observation time T [52]. Although, for the case of pure $1/f$ noise, the dependence on T is logarithmically slow, and barely noticeable. Nevertheless, even if the process would be non-stationary, this should not have any impact on the estimate of Hooge's parameter as only $\bar{I}$ is impacted by the non-stationarity.

5. Conclusions

We have proposed a general model of $1/f$ noise in homogeneous semiconductors which is based on the trapping-detrapping process of individual charge carriers. In contrast to the many previous works, we have assumed that the detrapping rate of each trapping center is random. We have shown that, if detrapping process obeys Arrhenius law (which is well-established empirically [48–51]), and if the vacant trap depths follow Boltzman distribution (which is also supported by experimental works [44–47]), the detrapping rate distribution will be uniform. When detrapping rates are uniformly distributed, a power-law distribution of the detrapping times equation (7) is obtained. It arises from the superposition of exponential detrapping time distributions representing contributions of the individual trapping centers with their own fixed detrapping rates (see figure 2).

Consequently, regardless of the exact details of the trapping process, as long as the trapping process is slow in comparison to the detrapping process, pure $1/f$ noise in a form of Hooge's empirical relation is obtained, equation (30). Corresponding expression of the Hooge's parameter, α_{H}, is then found to be a ratio between the rate parameters of the trapping and the detrapping processes, equation (29). The proportionality between the Hooge's parameter and the trapping rate was reported in previous experimental works [53–55], thus providing partial experimental verification for the Hooge's parameter expression we have derived from general theoretical considerations. Inverse proportionality between the Hooge's parameter and the maximum detrapping rate suggests interesting implications for approaching suppression of $1/f$ noise problem [68–70]. When the Arrhenius law applies, maximum detrapping rate could be increased either by manipulating the pre-exponential factor, or by decreasing shalowest trap depth (minimum activation energy) from which the Boltzmann distribution applies to the trap depth distribution. The obtained expression for the Hooge's parameter also suggests that $1/f$ noise arises from the temporal charge carrier number fluctuations, not from the spatial mobility fluctuations.

In section 3, we have discussed the implications of finite experiments. We have shown that the power spectral density may exhibit spurious low-frequency cutoff simply due to finite duration of the experiment or simulation. The obtained width of the cutoff is of the same order of magnitude as $\frac{\gamma_{\text{max}}}{\gamma_\theta}$. This cutoff disappears when the power spectral density is averaged over a large number of experiments, or when the experiment involves a large number of independent charge carriers. In the latter case the distribution of the signal's amplitude follows Binomial distribution, which under imperfect observation will quickly become indistinguishable from the Gaussian distribution.

Data availability statement

All of the code used to perform the reported numerical simulations is available at https://github.com/akononovicius/flicker-trap-detrap-individual-charge.

Author contributions

AK: Software, Validation, Writing—Original Draft, Writing—Review & Editing, Visualization. **BK:** Conceptualization, Methodology, Writing—Original Draft, Writing—Review & Editing.

References

[1] Johnson J B 1925 The Schottky effect in low frequency circuits *Phys. Rev.* **26** 71–85
[2] Schottky W 1926 Small-shot effect and flicker effect *Phys. Rev.* **28** 74–103
[3] Milotti E 2002 $1/f$ noise: a pedagogical review (arXiv:physics/0204033 [physics.class-ph])
[4] Kogan S 1996 *Electronic Noise and Fluctuations in Solids* (Cambridge University Press)
[5] Lowen S B and Teich M C 2005 *Fractal-Based Point Processes* (Wiley)
[6] van Kampen N G 2007 *Stochastic Process in Physics and Chemistry* (North Holland)
[7] Voss R F and Clarke J 1976 $1/f$ noise from systems in thermal equilibrium *Phys. Rev. Lett.* **36** 42–45
[8] Dutta P and Horn P M 1981 Low-frequency fluctuations in solids: $1/f$ noise *Rev. Mod. Phys.* **53** 497–516
[9] Mitin V, Reggiani L and Varani L 2002 Generation-recombination noise in semiconductors *Noise and Fluctuation Controls in Electronic Devices* (American Scientific Publishers)
[10] Balandin A A 2013 Low-frequency $1/f$ noise in graphene devices *Nat. Nanotechnol.* **8** 549–55
[11] Fox Z R, Barkai E and Krapf D 2021 Aging power spectrum of membrane protein transport and other subordinated random walks *Nat. Commun.* **12** 6162
[12] Wirth G, da Silva M B and Both T H 2021 Unified compact modeling of charge trapping in $1/f$ noise, RTN and BTI *2021 5th IEEE Electron Devices Technology and Manufacturing Conf. (EDTM)* (IEEE) pp 1–3
[13] Voss R F and Clarke J 1975 $1/f$ noise in music and speech *Nature* **258** 317–8
[14] Kobayashi M and Musha T 1982 $1/f$ fluctuation of heartbeat period *IEEE Trans. Biomed. Eng.* **29** 456–7
[15] Gilden D L, Thornton T and Mallon M W 1995 $1/f$ noise in human cognition *Science* **267** 1837–9
[16] Levitin D J, Chordia P and Menon V 2012 Musical rhythm spectra from Bach to Joplin obey a $1/f$ power law *Proc. Natl Acad. Sci. USA* **109** 3716–20
[17] Bernamont J 1937 Fluctuations in the resistance of thin films *Proc. Phys. Soc.* **49** 138–9
[18] Surdin M 1951 Une théorie des fluctuations électriques dans les semi-conducteurs *J. Phys. Radium* **12** 777–83
[19] McWhorter A L and Kingston R H 1957 Semiconductor surface physics *Proc. Conf. on Physics of Semiconductor Surface Physics* vol 207 (University of Pennsylvania)
[20] Ziel A V D 1979 Flicker noise in electronic devices *Advances in Electronics and Electron Physics* (Elsevier) pp 225–97
[21] Kaulakys B, Gontis V and Alaburda M 2005 Point process model of $1/f$ noise vs a sum of Lorentzians *Phys. Rev.* E **71** 051105
[22] Wong H 2003 Low-frequency noise study in electron devices: review and update *Microelectron. Reliab.* **43** 585–99
[23] Ruseckas J, Kaulakys B and Gontis V 2011 Herding model and $1/f$ noise *Europhys. Lett.* **96** 60007
[24] Kononovicius A and Gontis V 2012 Agent based reasoning for the non-linear stochastic models of long-range memory *Physica* A **391** 1309–14
[25] Kaulakys B and Alaburda M 2009 Modeling scaled processes and $1/f^{\beta}$ noise using non-linear stochastic differential equations *J. Stat. Mech.* P02051
[26] Kazakevicius R, Kononovicius A, Kaulakys B and Gontis V 2021 Understanding the nature of the long–range memory phenomenon in socioeconomic systems *Entropy* **23** 1125
[27] Ruseckas J and Kaulakys B 2014 Scaling properties of signals as origin of $1/f$ noise *J. Stat. Mech.* P06005
[28] Kaulakys B, Alaburda M and Ruseckas J 2015 $1/f$ noise from the nonlinear transformations of the variables *Mod. Phys. Lett.* B **29** 1550223
[29] Eliazar I 2021 Selfsimilar diffusions *J. Phys. A: Math. Theor.* **54** 35LT01

J. Stat. Mech. (2024) 113201

[30] Kazakevičius R and Kononovicius A 2023 Anomalous diffusion and long-range memory in the scaled voter model *Phys. Rev.* E **107** 024106
[31] Mandelbrot B B 2013 *Multifractals and $1/f$ Noise: Wild Self-Affinity in Physics (1963–1976)* (Springer)
[32] Beran J 2017 *Statistics for Long-Memory Processes* (Routledge)
[33] Giraitis L, Leipus R and Surgailis D 2009 ARCH(∞) models and long memory *Handbook of Financial Time Series* ed T G Anderson, R A Davis, J Kreis and T Mikosh (Springer) pp 71–84
[34] Bollerslev T 2023 The story of GARCH: a personal odyssey *J. Econom.* **234** 96–100
[35] Hooge F N 1969 $1/f$ noise is no surface effect *Phys. Lett.* A **29** 139–40
[36] Hooge F N 1972 Discussion of recent experiments on $1/f$ noise *Physica* **60** 130–44
[37] Hooge F N 1994 $1/f$ noise sources *IEEE Trans. Electron Devices* **41** 1926–35
[38] Kaulakys B 1999 Autoregressive model of $1/f$ noise *Phys. Lett.* A **257** 37–42
[39] Dmitriev A P, Levinshtein M E and Rumyantsev S L 2009 On the Hooge relation in semiconductors and metals *J. Appl. Phys.* **106** 024514
[40] Vandamme L K J 2013 How useful is Hooge's empirical relation *22nd Int. Conf. on Noise and Fluctuations (ICNF)* (IEEE) pp 1–6
[41] Palenskis V and Maknys K 2015 Nature of low-frequency noise in homogeneous semiconductors *Sci. Rep.* **5** 18305
[42] Gruneis F 2019 An alternative form of Hooge's relation for $1/f$ noise in semiconductor materials *Phys. Lett.* A **383** 1401–9
[43] Gruneis F 2022 $1/f$ noise under drift and thermal agitation in semiconductor materials *Physica* A **593** 126917
[44] Bisquert J 2008 Beyond the quasistatic approximation: impedance and capacitance of an exponential distribution of traps *Phys. Rev.* B **77** 235203
[45] Wong J, Omelchenko S T and Atwater H A 2020 Impact of semiconductor band tails and band filling on photovoltaic efficiency limits *ACS Energy Lett.* **6** 52–57
[46] Beckers A, Beckers D, Jazaeri F, Parvais B and Enz C 2021 Generalized Boltzmann relations in semiconductors including band tails *J. Appl. Phys.* **129** 045701
[47] Zeiske S, Sandberg O J, Zarrabi N, Li W, Meredith P and Armin A 2021 Direct observation of trap-assisted recombination in organic photovoltaic devices *Nat. Commun.* **12** 3603
[48] Peters B 2015 Common features of extraordinary rate theories *J. Phys. Chem.* B **119** 6349–56
[49] Kurpiers J *et al* 2018 Probing the pathways of free charge generation in organic bulk heterojunction solar cells *Nat. Commun.* **9** 2038
[50] Arakawa K *et al* 2020 Quantum de-trapping and transport of heavy defects in tungsten *Nat. Mater.* **19** 508–11
[51] Kumar V, Pal A and Shpielberg O 2024 Arrhenius law for interacting diffusive systems *Phys. Rev.* E **109** l032101
[52] Kononovicius A and Kaulakys B 2023 $1/f$ noise from the sequence of nonoverlapping rectangular pulses *Phys. Rev.* E **107** 034117
[53] Lukyanchikova N, Petrichuk M V, Garbar N P, Saščiuk A P and Kropman D I 1990 $1/f$ noise and generation-recombination processes at discrete levels in semiconductors *Physica* B **167** 201–7
[54] Tacano M, Pavelka J, Tanuma N, Yokokura S and Hashiguchi S 2004 Dependence of Hooge constant on mean free paths of materials *Fluctuations and Noise in Materials* ed D Popovic, M B Weissman and Z A Racz (SPIE) pp 310–9
[55] Tousek J, Touskova J and Krivka I 2024 Product of mobility and lifetime of charge carriers in cdte determined from low-frequency current fluctuations *Sci. Rep.* **14** 899
[56] Margolin G and Barkai E 2006 Nonergodicity of a time series obeying Levy statistics *J. Stat. Phys.* **122** 137–67
[57] Lukovic M and Grigolini P 2008 Power spectra for both interrupted and perennial aging processes *J. Chem. Phys.* **129** 184102
[58] Niemann M, Kantz H and Barkai E 2013 Fluctuations of $1/f$ noise and the low-frequency cutoff paradox *Phys. Rev. Lett.* **110** 140603
[59] Leibovich N, Dechant A, Lutz E and Barkai E 2016 Aging Wiener-Khinchin theorem and critical exponents of $1/f^{\beta}$ noise *Phys. Rev.* E **94** 052130
[60] Frantsuzov P, Kuno M, Jankó B and Marcus R A 2008 universal emission intermittency in quantum dots, nanorods and nanowires *Nat. Phys.* **4** 519–22
[61] Cordones A A and Leone S R 2013 Mechanisms for charge trapping in single semiconductor nanocrystals probed by fluorescence blinking *Chem. Soc. Rev.* **42** 3209
[62] Nenashev A V, Valkovskii V V, Oelerich J O, Dvurechenskii A V, Semeniuk O, Reznik A, Gebhard F and Baranovskii S D 2018 Release of carriers from traps enhanced by hopping *Phys. Rev.* B **98** 155207
[63] Haneef H F, Zeidell A M and Jurchescu O D 2020 Charge carrier traps in organic semiconductors: a review on the underlying physics and impact on electronic devices *J. Mater. Chem.* **8** 759–87
[64] Gentle J E 2009 Mathematical and statistical preliminaries *Statistics and Computing* (Springer) pp 5–79

[65] Melkonyan S V 2010 Non-Gaussian conductivity fluctuations in semiconductors *Physica* B **405** 379–85
[66] Ruseckas J, Kazakevicius R and Kaulakys B 2016 Coupled nonlinear stochastic differential equations generating arbitrary distributed observable with $1/f$ noise *J. Stat. Mech.* 043209
[67] Leibovich N and Barkai E 2017 Conditional $1/f^{\alpha}$ noise: from single molecules to macroscopic measurement *Phys. Rev.* E **96** 032132
[68] Kamada M, Zeng W, Laitinen A, Sarkar J, Yeh S-S, Tappura K, Seppä H and Hakonen P 2023 Suppression of $1/f$ noise in graphene due to anisotropic mobility fluctuations induced by impurity motion *Commun. Phys.* **6** 207
[69] Nakatani T, Suto H, Kulkarni P D, Iwasaki H and Sakuraba Y 2023 Improvement of magnetic field detectivity in electrical $1/f$ noise-dominated tunnel magnetoresistive sensors by AC magnetic field modulation technique *J. Appl. Phys.* **134** 213904
[70] Balandin A A, Paladino E and Hakonen P J 2024 Electronic noise—from advanced materials to quantum technologies *Appl. Phys. Lett.* **124** 050401